Tectonophysics 657 (2015) 205–218

Contents lists available at ScienceDirect

Tectonophysics

journal homepage: www.elsevier.com/locate/tecto

Active upper crust deformation pattern along the southern edge of the Tyrrhenian subduction zone (NE Sicily): Insights from a multidisciplinary approach

Mimmo Palano [a,*], Domenico Schiavone [b], Mariano Loddo [b], Marco Neri [a], Debora Presti [c], Ruggiero Quarto [b], Cristina Totaro [c], Giancarlo Neri [c]

[a] Istituto Nazionale di Geofisica e Vulcanologia, Osservatorio Etneo—Sezione di Catania, Catania, Italy
[b] Dipartimento di Scienze della Terra e Geoambientali, Università di Bari, Bari, Italy
[c] Dipartimento di Fisica e di Scienze della Terra, Università di Messina, Messina, Italy

ARTICLE INFO

Article history:
Received 22 July 2014
Received in revised form 1 July 2015
Accepted 3 July 2015
Available online 17 July 2015

Keywords:
Subduction edge
Seismic velocity structure
Density model
Ground deformation
Crustal shear zone
Calabro-Peloritan Arc

ABSTRACT

Using a multidisciplinary dataset based on gravimetric, seismic, geodetic and geological observations, we provide an improved picture of the shallow structure and dynamics of the southern edge of the Tyrrhenian subduction zone. With a local earthquake tomography we clearly identify two main crustal domains in the upper 15 km characterized by different P-wave velocity values: a high-velocity domain comprising southeasternmost Tyrrhenian Sea, NE Sicily and Messina Straits, and a low-velocity domain comprising Mt. Etna and eastern Sicily. The transition between the two domains shows a good spatial correspondence with a wider set of faults including the Taormina Fault System (TFS) and the Aeolian–Tindari–Letojanni Fault System (ATLFS), two nearly SE-striking fault systems crossing northeastern Sicily and ending on the Ionian shoreline of Sicily according to many investigators. Within this set of faults, most of the deformation/seismicity occurs along the northern and central segments of ATLFS, compared to low activity along TFS. A lack of seismicity (both recent and historical) is observed in the southern sector of ATLFS where, however, geodetic data reveal significant deformation. Our multidisciplinary dataset including offshore observations suggests the southeastward continuation of the ATLFS into the Ionian Sea until joining with the faults cutting the Ionian accretionary wedge described in the recent literature. Our findings imply the existence of a highly segmented crustal shear zone extending from the Aeolian Islands to the Ionian Abyssal plain, that we believe plays the role of accommodating differential motion between the Southern Tyrrhenian unit and the western compressional domain of Sicily. The ATLFS, which is a main part of the inferred shear zone, behaves similarly to what often observed at the edges of retreating subduction slabs, where the overriding plate drifts with a highly non-uniform transform motion along the lateral borders.

1. Introduction

At present, the Central Mediterranean basin is dominated by the geodynamic processes related to (i) the convergence between the African and the Eurasian plates (e.g. Malinverno and Ryan, 1986) and (ii) active back-arc spreading in the hanging-wall of the Apennines subduction zone (e.g. Cuffaro et al., 2011). Geological, seismological and geodetic observations collected in the past few decades in southern Italy have provided evidence that active crustal shortening is widely accommodated in southeastern Sicily at the front of the Apennine–Maghrebian orogen and along the northern-western offshore of Sicily (Fig. 1; Goes et al., 2004; Pondrelli et al., 2004; Palano et al., 2012; Presti et al., 2013). In southeastern Sicily the convergence process caused the segmentation of the Hyblean foreland by the reactivation of pre-existing structures (Musumeci et al., 2014), while along the northern-western offshore of Sicily the crustal shortening occurs along thrusts whose fronts are laterally offset by newly formed right-lateral crustal shear zones (Billi et al., 2007; Goes et al., 2004; Pondrelli et al., 2004). In northeastern Sicily and southern Calabria, crustal extension is controlled by subduction underneath the Calabro-Peloritan Arc of the Ionian oceanic crust and by southeast directed rollback of the subducting slab (see Neri et al., 2012 and references therein). The different deformation patterns of the two main geodynamic domains of the Western-Central Sicily and the Calabro-Peloritan Arc are accommodated in northeastern Sicily and several researchers (e.g. Billi et al., 2006; Cuffaro et al., 2011; Palano et al., 2012) have suggested that in this area a major role is played by the so called "Aeolian–Tindari–Letojanni" Fault System (hereinafter ATLFS), a complex and heterogeneous crustal discontinuity consisting of a broad NNW–SSE- to NW–SE-trending system of faults running from

* Corresponding author at: Istituto Nazionale di Geofisica e Vulcanologia, Osservatorio Etneo—Sezione di Catania, P.zza Roma, 2, 95123 Catania, Italy. Tel.: +39 095 7165800.
E-mail address: mimmo.palano@ingv.it (M. Palano).

http://dx.doi.org/10.1016/j.tecto.2015.07.005
0040-1951/

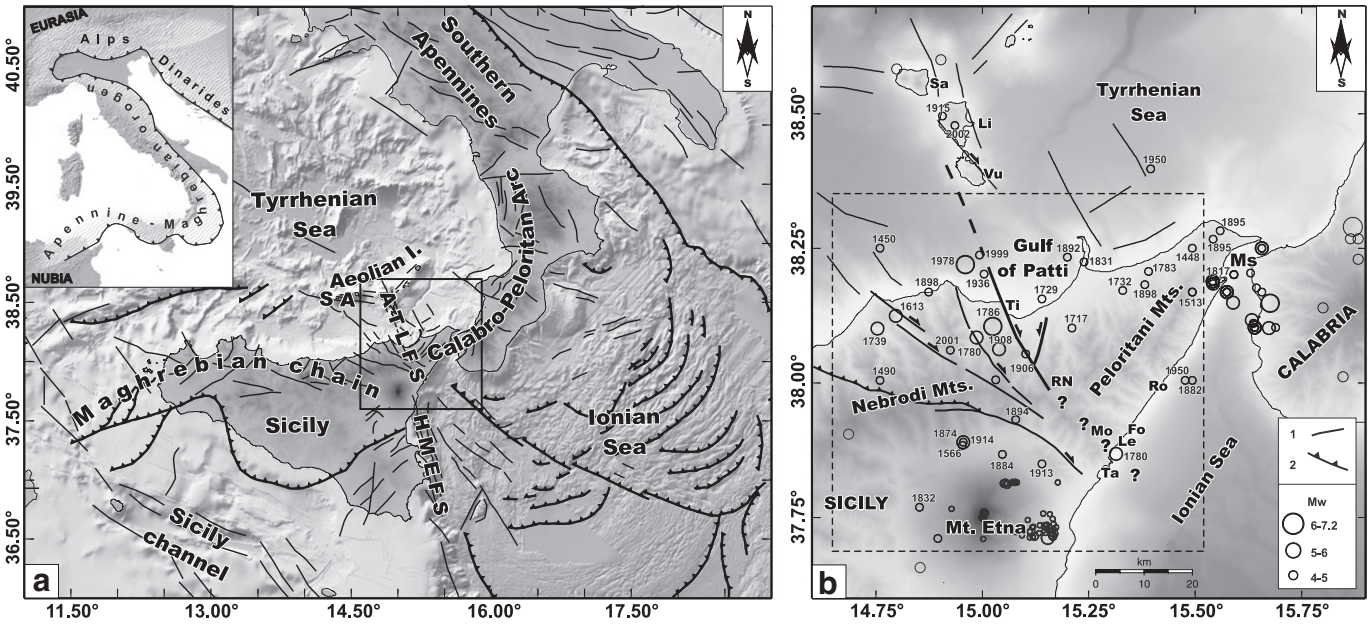

Fig. 1. a) Simplified tectonic map of Sicily and surrounding areas. Abbreviations are: ATLFS, Aeolian–Tindari–Letojanni Fault System; TFS, Tindari Fault System; HMEFS, Hyblean–Maltese Escarpment Fault System; SA, Sisifo–Alicudi shear zone. The Maghrebian Chain and the Calabro Peloritan Arc are parts of the Apennine–Maghrebian orogen (see inset). The black rectangle encloses the area reported in panel b). b) Circles show the locations of the earthquakes that have occurred in the investigated area after 1000 A.D. according to the CPTI11 catalogue (Rovida et al., 2011; http://emidius.mi.ingv.it/CPTI11). Labels indicate the year of occurrence. The completeness magnitude of the catalogue is 6.4, 5.9, 5.2 and 4.7 since 1300, 1530, 1700 and 1895, respectively (http://zonesismiche.mi.ingv.it). Epicentres falling in the Mt. Etna area and the Messina Straits are not labelled. Fo = Forza D'Agrò; Le = Letojanni; Li = Lipari; Ms = Messina Strait; Mo = Mongiuffi; RN = Rocca Novara; Ro = Roccalumera; Sa = Salina; Ta = Taormina; Ti = Tindari; Vu = Vulcano. Major oblique dip–slip (1) and reverse (2) faults are also reported. The dashed rectangle indicates the main study area of the present work.

the Aeolian Islands down to the Ionian coast of Sicily (Fig. 1). Notwithstanding that the ATLFS is characterized by the lack of tectonic and morphological faulting expressions at its southern termination (Fig. 1; e.g. Billi et al., 2006; De Guidi et al., 2013), several authors extend it down to the Ionian coast of Sicily, linking it with major tectonic structures located close to the Ionian offshore. Several investigators connect the ATLFS with the Hyblean–Maltese Escarpment fault system (e.g. Govers and Wortel, 2005; Lanzafame and Bousquet, 1997; Rosenbaum et al., 2008), a right lateral transtensional Mesozoic lithospheric boundary separating the Sicilian continental crust from the Ionian oceanic basin (Fig. 1a). Other investigators suggest that ATLFS simply connects the northern-western Sicilian contractional belt to the Ionian accretionary wedge, accommodating differential movements within the contractional belt itself (Fig. 1a; e.g. Goes et al., 2004; Neri et al., 2004; Billi et al., 2006). A number of authors (e.g. Govers and Wortel, 2005; Neri et al., 2009; Rosenbaum et al., 2008 and references therein) suggest the ATLFS is the current shallow expression of a sub-vertical lithospheric-scale tear-fault, bordering the southern edge of the Tyrrhenian subduction zone at depth. Other investigators advocate that ATLFS developed during the Plio-Pleistocene as part of a complex synthetic and antithetic grid of high-angle strike–slip faults and is no longer active (e.g. Catalano et al., 2009; Giunta et al., 2009).

This study focuses on the ATLFS and surrounding zones. We adopted a multidisciplinary approach based on gravimetric, seismic, geodetic and geological observations collected in the last two decades. In particular, we have investigated a broad deformation zone that include the ATLFS and attempted to establish whether such a deformation zone really play the role of accommodating the differential motion between the eastern extensional domain of the Calabro-Peloritan Arc and the western compressional one of Western-Central Sicily.

2. Background setting

The convergence between the African and Eurasian plates has dominated the evolution of the central Mediterranean basin since the Cretaceous, controlling the generation, spatial distribution and shape of all mountain chains and of the intervening basins (Anderson and Jackson, 1987; Dewey et al., 1973; Doglioni, 1993; Jolivet et al., 1998). Despite the convergence process occurring at a rate of 1–2 cm/yr during the last 8–10 Myr, the Calabro-Peloritan Arc (part of the Apennine–Maghrebian orogen accreted since the Miocene; Fig. 1a, Malinverno and Ryan, 1986; Patacca et al., 1990), experienced rapid E to SE motion at a rate of 5–8 cm/yr up to Early Pleistocene, driven by rollback of the Ionian subducting slab. Moreover, during the Middle–Late Pleistocene, when the Calabro-Peloritan Arc almost reached its present location, subduction trench retreat slowed to less than 1 cm/yr, probably because of a tectonic reorganization on this sector of the Mediterranean basin (Faccenna et al., 2001; Goes et al., 2004; Westaway, 1990; Wortel and Spakman, 2000). Regional tectonic evolution and lithospheric structures were strongly influenced by rollback and back-arc extension, with the formation of new oceanic crust in the Tyrrhenian Sea basin (Faccenna et al., 2004; Gueguen et al., 1998; Rosenbaum and Lister, 2004). The progressive southeastward rollback of the subducting slab was accommodated by the development of some right-lateral shear zones which, bordering the forearc–backarc system, have migrated eastward over time (e.g. Billi et al., 2010; Finetti et al., 1996; Rosenbaum and Lister, 2004). The NNW–SSE striking Aeolian–Tindari–Letojanni Fault System (ATLFS), consisting of a set of mainly right-lateral and extensional faults (Fig. 1b), is believed to represent the easternmost and youngest of these tectonic accommodation structures (Finetti et al., 1996; Guarnieri, 2006).

The ATLFS can be divided into three sectors (northern, central and southern) characterized by different kinematic, geological and geomorphological features. The northern sector extends from the central Aeolian Islands up to the Gulf of Patti. The central sector develops in northeastern Sicily onshore, between Tindari and the watershed of the Peloritani Mts. (close to Rocca Novara; RN in Fig. 1b), while the southern sector extends from the watershed of the Peloritani Mts. down to the Ionian coast, close to Letojanni (Le in Fig. 1b). The ATLFS is rather well defined by geological and geophysical evidences only in its northern and central sectors, while in the southern sector it is characterized by less evident tectonic and morphological faulting expressions (Billi

et al., 2006; De Guidi et al., 2013). In this regard, some investigators report that the ATLFS does not extend across the Peloritani Mts. chain down to the Ionian coast and also suggest that it is no longer active (e.g. Argnani, 2014; Catalano et al., 2009; Giunta et al., 2009).

Northward, the ATLFS joints with the Sisifo–Alicudi structural system (Fig. 1a), a seismically active transpressional zone belonging to the overall east-trending convergent margin localized between the Ustica and Aeolian Islands (Billi et al., 2007; De Astis et al., 2003). The northern sector of ATLFS has been mapped by seismic reflection profiles, marine geology and bathymetric surveys carried out on the western side of the Salina–Lipari–Vulcano volcanic complex (e.g. De Astis et al., 2003; Favalli et al., 2005). This sector of ATLFS consists of NNW–SSE-trending faults following an en echelon pattern along two main branches bordering the western and eastern flanks of Vulcano, cutting the south-western flank of Lipari and Salina and extending southward in the Gulf of Patti area (e.g. Argnani et al., 2007; Favalli et al., 2005; Ventura et al., 1999). Secondary N–S and NE–SW striking faults, mapped on-land, accommodate the right-lateral component of the main NNW–SSE strike–slip faults. Evidence of neotectonic activity of these segments of ATLFS, as well as of the segments cutting the Gulf of Patti area, is also inferred by the occurrence of low-to-moderate earthquakes with prevailing right-lateral slip on NNW–SSE-striking fault planes (Gambino et al., 2012; Neri et al., 2005).

The central sector of the ATLFS consists of a NNW–SSE-striking set of faults, cutting both the Cretaceous–Miocene sedimentary and the Hercynian metamorphic units of the orogenic arc (see Figure S1 in the Supplementary material section). These fault segments are characterized by steeply inclined scarps (dip ≥ 60°) mainly eastward dipping with dominant dip–slip kinematics and secondary right-lateral ones (Ghisetti, 1979; Billi et al., 2006; De Guidi et al., 2013, see also Fig. 8b). East of the central segment of ATLFS, on the north side of the Peloritani Mts., a second-order N–S- and NE–SW-striking fault system with dip–slip and left oblique kinematics can also be recognized (Fig. 1b and Fig. 8a). Southwards, across the Peloritani Mts., the geological and geomorphological evidence of neotectonic activity of the ATLFS is substantially lacking due to the extensive outcropping of low- to middle-grade metamorphic rocks belonging to the Hercynian basement (Ghisetti, 1979). Close to the Ionian coast (e.g. Forza D'Agrò, Mongiuffi; Fig. 1b), the outcropping of allochthonous sedimentary successions allows identifying some short fault segments characterized by prevailing Pleistocene–Holocene dip–slip and right-lateral kinematics on planes with N110°–170°E attitude (Ghisetti, 1979; see also Fig. 8d as an example). These faults were interpreted as the southern edge of the ATLFS (e.g. Billi et al., 2006; Lanzafame and Bousquet, 1997; Rosenbaum et al., 2008) even though the lack of clear traces of neotectonic activity in the area comprised between Mongiuffi and Rocca Novara (Mo and RN in Fig. 1b) raises some doubt on this interpretation (e.g. Argnani, 2014).

The catalog of historical earthquakes of Italy (Rovida et al., 2011) shows that the seismicity in the study area (Fig. 1b) has mainly occurred in a belt roughly corresponding to the ATLFS, and including several events with macroseismic estimated moment magnitude $M_W > 5$ and a maximum value of 6.2 (Azzaro et al., 2007). Along this belt, however, the already mentioned ATLFS sector comprised between Mongiuffi and Rocca Novara can clearly be distinguished for the absence of historical seismicity (Fig. 1b). It is worth pointing out that historical seismicity is fairly well documented in the study area (Rovida et al., 2011). Even accounting for the uncertainty of magnitudes and epicentre locations in this dataset, the lack of activity in the onshore zone between Mongiuffi and Rocca Novara is still highly significant (Azzaro et al., 2007; Neri et al., 2006).

3. Geophysical data

Investigation of the study area (dashed rectangle in Fig. 1b) has been done using an extensive dataset based on gravimetric, seismic and geodetic observations collected in the past two decades. In the following, we provide a brief description of each type of dataset used. Additional details on the data processing are reported in Appendix A of the Supplementary material.

3.1. Gravimetric data

Gravimetric measurements were carried out in the past decade in the study area on a dense gravimetric network of 807 stations with a mean station spacing of ~1 km (Fig. 2a). Gravimetric measurements were tied to the 1971 International Standardization Net (IGSN71; Morelli et al., 1974) and corrected for the 1980 International Gravity Formula (IGF; Moritz, 1980). Moreover, for each station, the so called "terrain correction" process was also applied (see Appendix A.1 of the Supplementary material for further details). The resulting Bouguer anomaly map is shown in Fig. 2b. Both contours and features of these anomalies match well with those reported in the gravimetric map of Italy (Ballarin et al., 1972), and improve the resolution over the investigated area thanks to the dense gravimetric network. For instance, the lowering of the anomaly values obtained in the southeastern side of the study area concurs with the minimum value evidenced by Ballarin

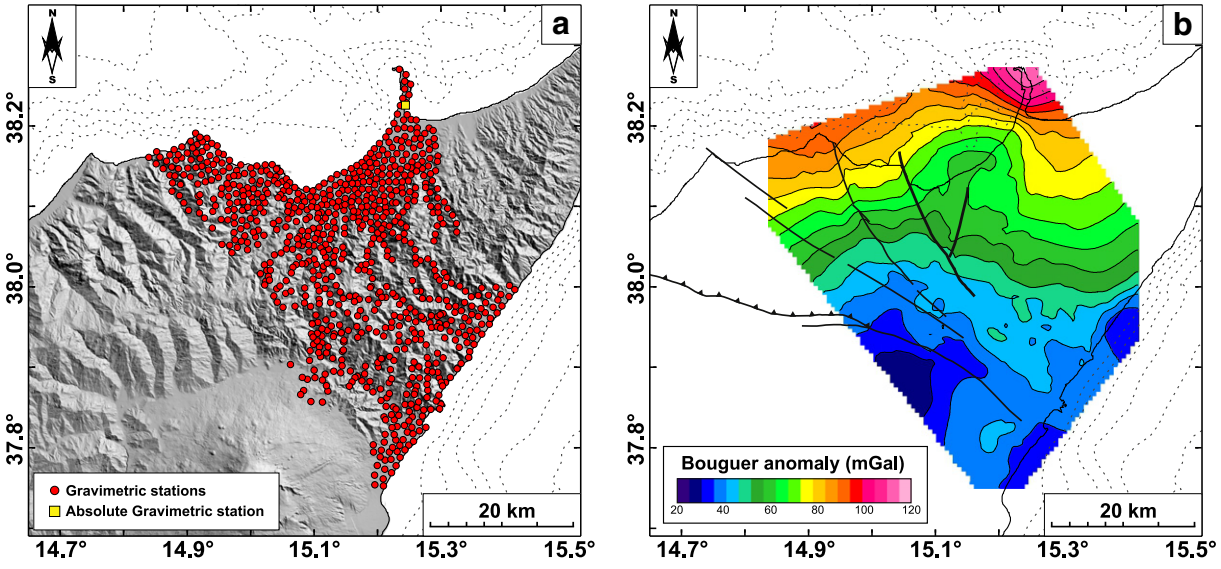

Fig. 2. a) Location of gravimetric stations in the investigated area. b) Resulting Bouguer anomalies; the contour interval is 5 mGal.

et al. (1972) for the area comprised between the Ionian and Calabrian coasts.

The data inversion was performed using the nonlinear approach described in Camacho et al. (2000, 2002, 2011) and subdividing the subsurface volume into prismatic bodies, slightly increasing their volume with depth. Results from the inversion are reported in Fig. 3 as horizontal slices at various depths of the modelled density contrast with respect to a reference density value (the "0" value in Fig. 3). Since we selected a solution with contrasts close to the limiting values for the inversion, we obtained a model with generally more compact anomalous bodies and with a sharp geometry that is better suited to detect critical zones. Fig. 3 clearly shows low density bodies in the southern part of the investigated area extending down to a depth of about 18 km and the presence of high density bodies located in the northern part of the area, characterizing the model down to 15 km. To correctly understand the model obtained by the inversion procedure, it should be kept in mind that the measurements represent the vertical component of the gravimetric attraction. Consequently, the sources of the anomalies shown in the Bouguer map are predominantly located in the volume beneath the area covered by the gravimetric stations. A simple comparison with the outcropping rocks (see Figure S1 of Supplementary material) allows associating, at least for the shallow depths, the low density values to the sedimentary successions (extensively outcropping in the southern sector of the investigated area) and the high density values

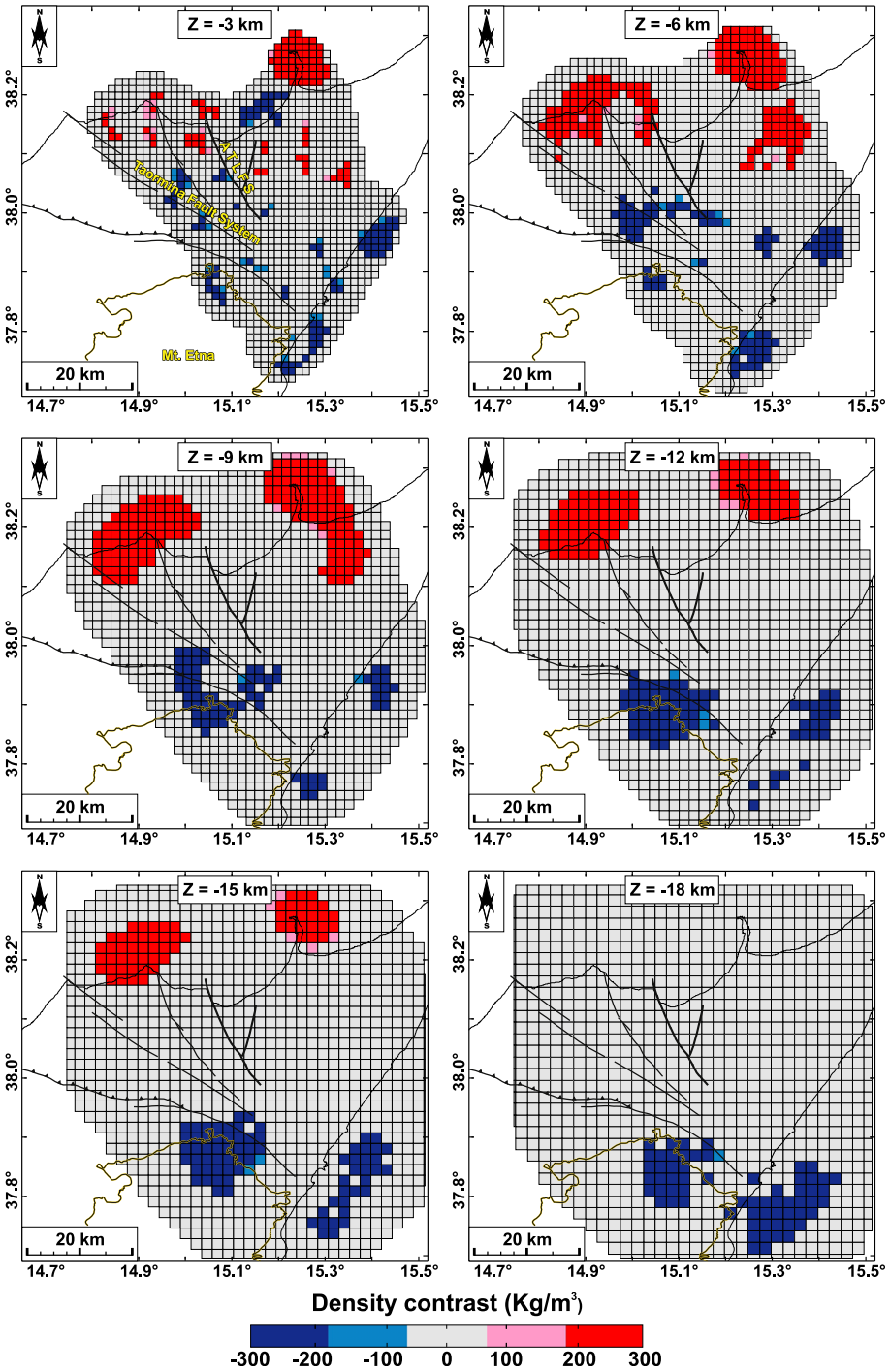

Fig. 3. Distribution of the recovered density model at different depth levels. The yellow line represents the boundary of the Mt. Etna volcano. The Taormina Fault System and the central sector of the Aeolian–Tindari–Letojanni Fault System (ATLFS) are also reported.

to metamorphic rocks, outcropping in the northeastern sector of the area.

3.2. Seismological data

Data and recordings relative to the shallower than 40 km earthquakes, occurring in northeastern Sicily and Southern Calabria between January 1981 and April 2012, have been taken from the Italian national catalogues and databases (www.ingv.it) and from the databases of the local seismic networks operating in Calabria and Sicily (see Orecchio et al., 2011 and references therein). The dataset selected for tomographic inversion consisted of 49893 P and 30930 S arrival times from 4920 earthquakes recorded at a total of 282 stations (see Fig. S4a of Supplementary material).

From the collected dataset, we selected all the earthquakes with a minimum of 7 P and 8 P + S readings, whose quality in the majority of cases was verified directly on the recordings. We used the standard Simulps code by Evans et al. (1994) to invert the arrival time data for the P-wave velocity structure in the 0–40 km depth range with horizontal and vertical grid spacing of 5 km (see Appendix A.2 of the Supplementary material for details on the data used and quality of inversion).

Fig. 4 shows the 3-D V_P model obtained in the best resolved depth range after inversion (0–25 km). In the upper 15 km, two main velocity domains can be distinguished: (i) a high velocity domain covering the southeasternmost part of the Tyrrhenian Sea, northeastern Sicily and Messina Straits; (ii) a low-velocity one in the south-western part of the study area corresponding to Mt. Etna and the eastern part of Sicily. In the frame of the high velocity domain, a low velocity anomaly can be noticed at least in the upper 5 km beneath the central Aeolian Islands (Vulcano, Lipari and Salina), probably related to the local volcanism. At the depth levels of 20 and 25 km, a low-velocity belt running E–W from Sicily to the southern part of Messina Straits can clearly be distinguished.

Fig. 5a displays the earthquake locations obtained by the simultaneous inversion leading to the tomographic model of Fig. 4. The map shows the crustal seismicity (depth ≤ 25 km) distribution and includes ~3400 events with local magnitude ranging between 2.0 and 4.8. The highest level of activity is in the Mt. Etna area. Remarkable levels of seismic activity can also be noted west of the central Aeolian Islands and along the northern and central sectors of the ATLFS (between the Vulcano Island and Peloritani Mts. in northeastern Sicily; Fig. 5a). The seismicity drops to almost to nil in the southern sector of the ATLFS, between the already mentioned villages of Rocca Novara and Mongiuffi (Fig. 1b and Fig. 5a). Moving southeastward, along the projected continuation of the ATLFS in the Ionian Sea, some level of seismic activity can again be detected, showing a clear NW–SE trend of the epicentre distribution. Other clusters of events may also be detected in the western side of the investigated area and in southern Calabria.

To investigate the seismic deformation pattern we have reported in Fig. 5b the database of earthquake fault plane solutions (FPSs) compiled with data from public catalogues (www.globalcmt.org; www.bo.ingv.it/RCMT/searchRCMT.html) and from the literature (De Guidi et al., 2013; Frepoli and Amato, 2000; Gambino et al., 2012; Giammanco et al., 2008; Neri et al., 2003, 2005; Orecchio et al., 2014; Presti et al., 2013). Since in the study area the waveform-inversion focal solutions have proven much better constrained than solutions obtained by first-motion polarity inversion (e.g. D'Amico et al., 2010; Pondrelli et al., 2006; Scognamiglio et al., 2009), we have chosen to report in Fig. 5b the former when both types of solutions were available for the same earthquake. Examining the spatial distribution of the collected FPSs, we may observe that the northern sector of ATLFS is prevailingly characterized by right-lateral strike–slip faulting on NNW-trending dislocation planes parallel to the main fault system. To the south, along the central sector of the ATLFS (between Tindari and the watershed of Peloritani Mts.), the dominant deformation style is normal faulting on NE-oriented dislocation planes and, therefore, rotated with respect to the NNW–SSE ATLFS main trend. Southeastward, after the low-to-nil level of activity recorded in the southern sector of ATLFS (between the Peloritani Mts. and the Ionian coast of Sicily), seismic activity resumes again with right-lateral strike–slip and normal-faulting FPSs along the projected continuation of the ATLFS in the Ionian offshore (Fig. 5b).

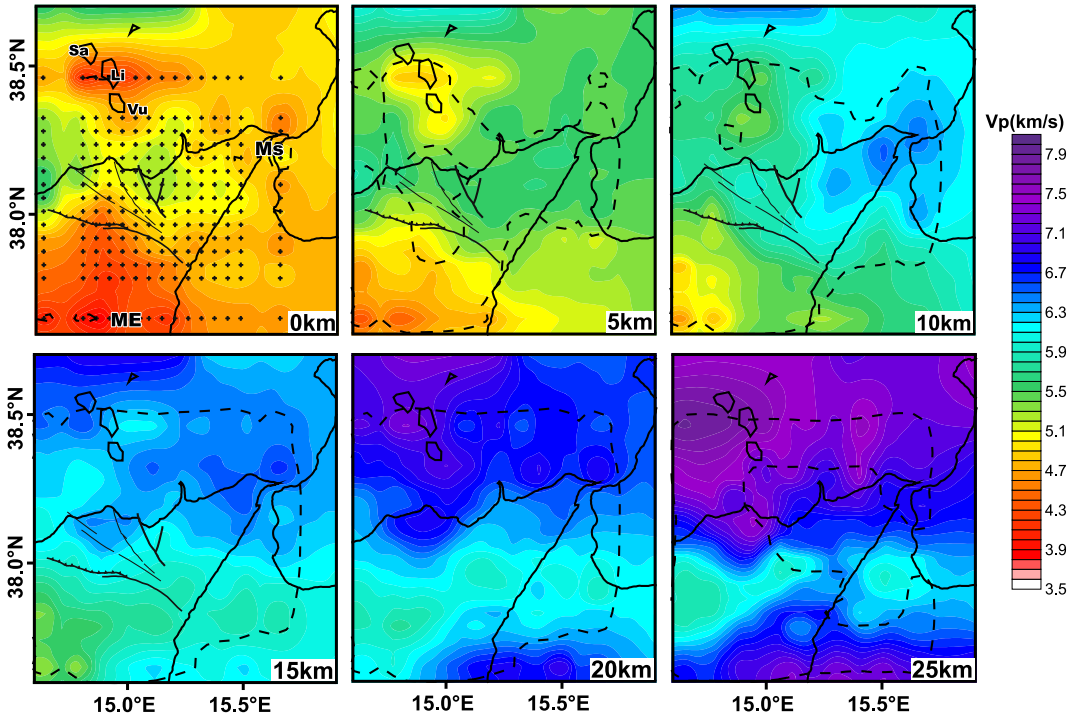

Fig. 4. P-wave velocity model from tomographic inversion performed in the present study. The number in the low right corner indicates the b.s.l. depth in kilometres. The black dashed curve contours the zone where the spread function (SF) values are smaller than 3.0. The main faults discussed in the study are also reported. The planimetric view of the inversion grid is displayed in the "0 km" map. Li = Lipari; Ms = Messina Strait; ME = Mount Etna; Sa = Salina; Vu = Vulcano.

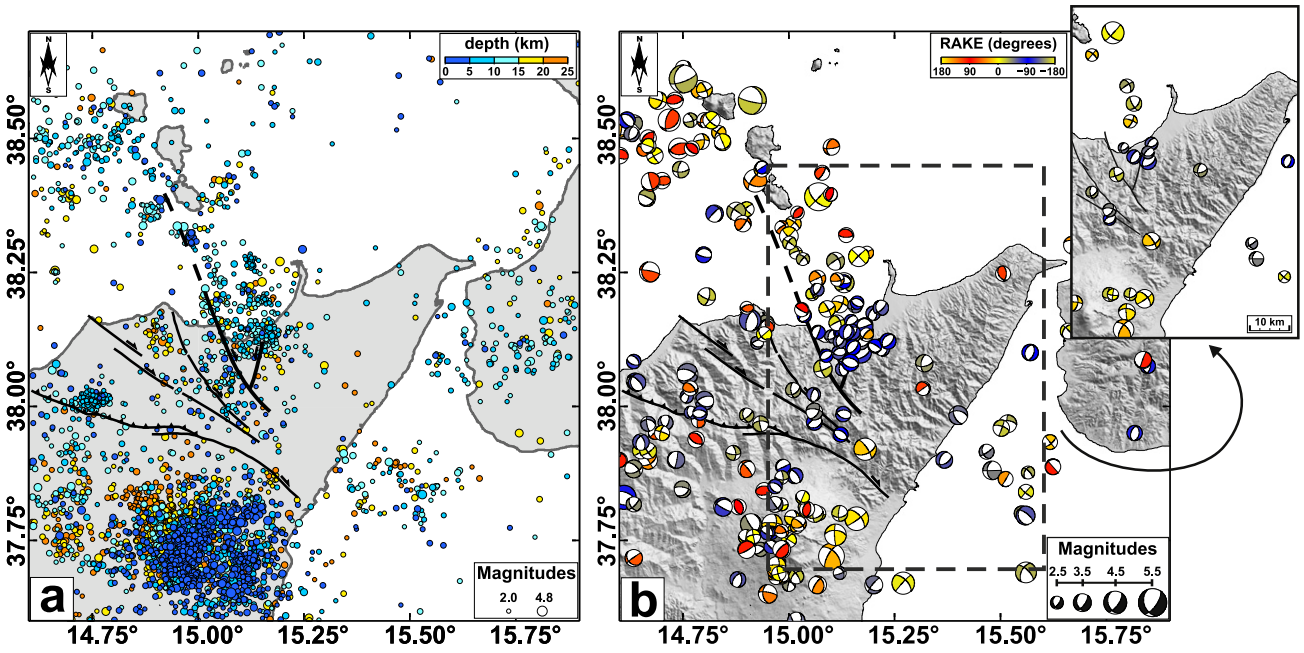

Fig. 5. a) Epicentre map of the earthquakes relocated in the local velocity structure computed in this study which occurred in the depth range of 0–25 km between January 1981 and April 2012 ($2 \le M \le 4.8$). Circles are proportional to magnitude and colour-coded according to hypocenter depths. Epicentre and focal depth uncertainties are in the order of 1.5 and 3 km, respectively. They have been estimated by Bayloc, the non-linear location method by Presti et al. (2004) capable of providing better location error estimates than linearized methods (Presti et al., 2008). b) Focal mechanisms of crustal earthquakes of magnitude $M \ge 2.5$ collected in the study (red, blue and yellow indicate reverse, normal and strike–slip faulting, respectively). In the top-right inset, only the best-quality mechanisms of our dataset computed by waveform inversion are reported.

Even with the drop in seismicity between the Peloritani Mts. and almost up to the Ionian coast of Sicily, the structural data of ATLFS and the earthquake locations/FPSs available between the central Aeolian Islands and the Ionian Sea offshore Letojanni seem to suggest a continuity (both structural and kinematic) of the ATLFS with the Ionian faults (Fig. 1a). The right-lateral transtensional behaviour of the ATLFS with its possible continuation in the Ionian Sea is further confirmed if we report only the best quality FPSs in the map, namely those estimated by waveform inversion (inset of Fig. 5b).

Finally, a remarkable level of mechanism heterogeneity can be noted in the highly active area of Mt. Etna volcano (Fig. 5b), while in the other zone of relatively intense seismicity, west of the central Aeolian Islands, transpressional faulting appears dominant and may be related to the action of the overall EW-trending convergent margin between Ustica and Aeolian Islands as found by previous investigators (e.g. Billi et al., 2007; Goes et al., 2004; Palano et al., 2012; Pondrelli et al., 2004; Presti et al., 2013).

3.3. Geodetic data

GNSS-based observations, collected over the investigated area during episodic measurement campaigns (1996–2008) as well as

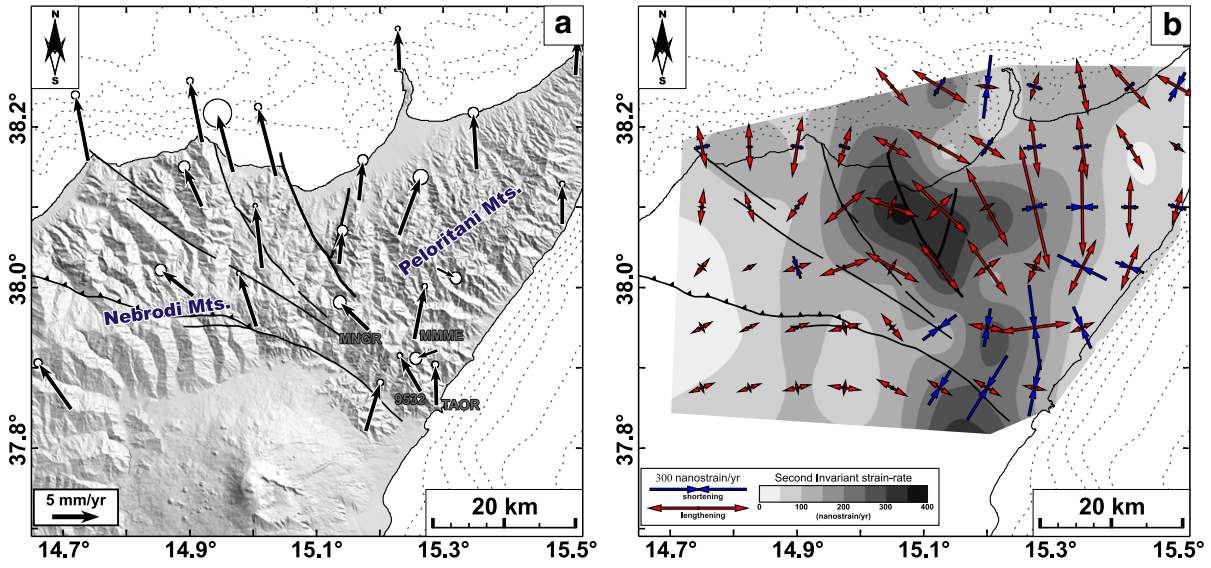

Fig. 6. a) GNSS velocities and 95% confidence ellipses in a fixed Eurasian reference frame. b) Geodetic strain-rate parameters: the colour in background shows the second invariant of the strain rate field, while arrows represent the greatest extensional ε_{Hmax} (red) and contractional ε_{hmin} (blue) horizontal strain-rates as computed at the nodes of each grid cell. MNGR, MMME, 9532 and TAOR are GNSS sites.

by continuous monitoring (since 2006), were processed using the GAMIT/GLOBK software packages (Herring et al., 2010) following the approach described in Palano (2015); see Appendix A.3 of the Supplementary material for additional details. To appropriately show the crustal deformation pattern, estimated GNSS velocities were aligned to a fixed Eurasian reference frame (Fig. 6a; Euler vector parameters: N55.963, E-97.169 and $\Omega = 0.262°$/My; Palano et al., 2013). Furthermore, assuming that the crust deforms as a continuum medium (e.g. England and Molnar, 1997), we computed the 2D strain-rate tensor over the studied area. In a first step, by taking the observed horizontal velocity field and associated covariance information into account, we derived a continuous velocity gradient tensor on a regular $0.075° \times 0.075°$ grid (whose nodes do not coincide with any of the GNSS stations) using a "spline in tension" technique (Wessel and Bercovici, 1998). The tension is controlled by a factor T, where $T = 0$ leads to a minimum curvature (natural bicubic spline), while $T = 1$ leads to a maximum curvature, allowing for maxima and minima only at observation points; we set $T = 0.4$ in our computations. We then computed the average 2D strain-rate tensor, its principal axes and the second invariant of tensor as derivative of the velocities at the nodes of each grid cell (Fig. 6b).

The geodetic velocity field is characterized by a general N-directed motion with a fan-shaped pattern. In detail, sites located on the Nebrodi and Peloritani mountain chains move toward NNW and NNE, respectively, evidencing a diverging pattern between the two sectors. To the southeast, the geodetic velocity pattern is more complicated due to a different motion of fairly close geodetic sites (Fig. 6a). The resulting strain-rate field (Fig. 6b) clearly evidences how the highest strain-rates (reported in terms of the second invariant of the strain rate tensor) are mainly concentrated in the central sector of ATLFS and in the area between the watershed of the Peloritani Mts. and the Ionian coastal area. The former is characterized by ε_{Hmax} axes with orientations ranging from NW–SE to N–S: because ε_{Hmax} is greater than ε_{hmin}, this area is characterized by an extensional strain field. In the latter, ε_{Hmax} and ε_{hmin} have similar magnitudes, indicating that deformation occurs under a shear-dominated regime.

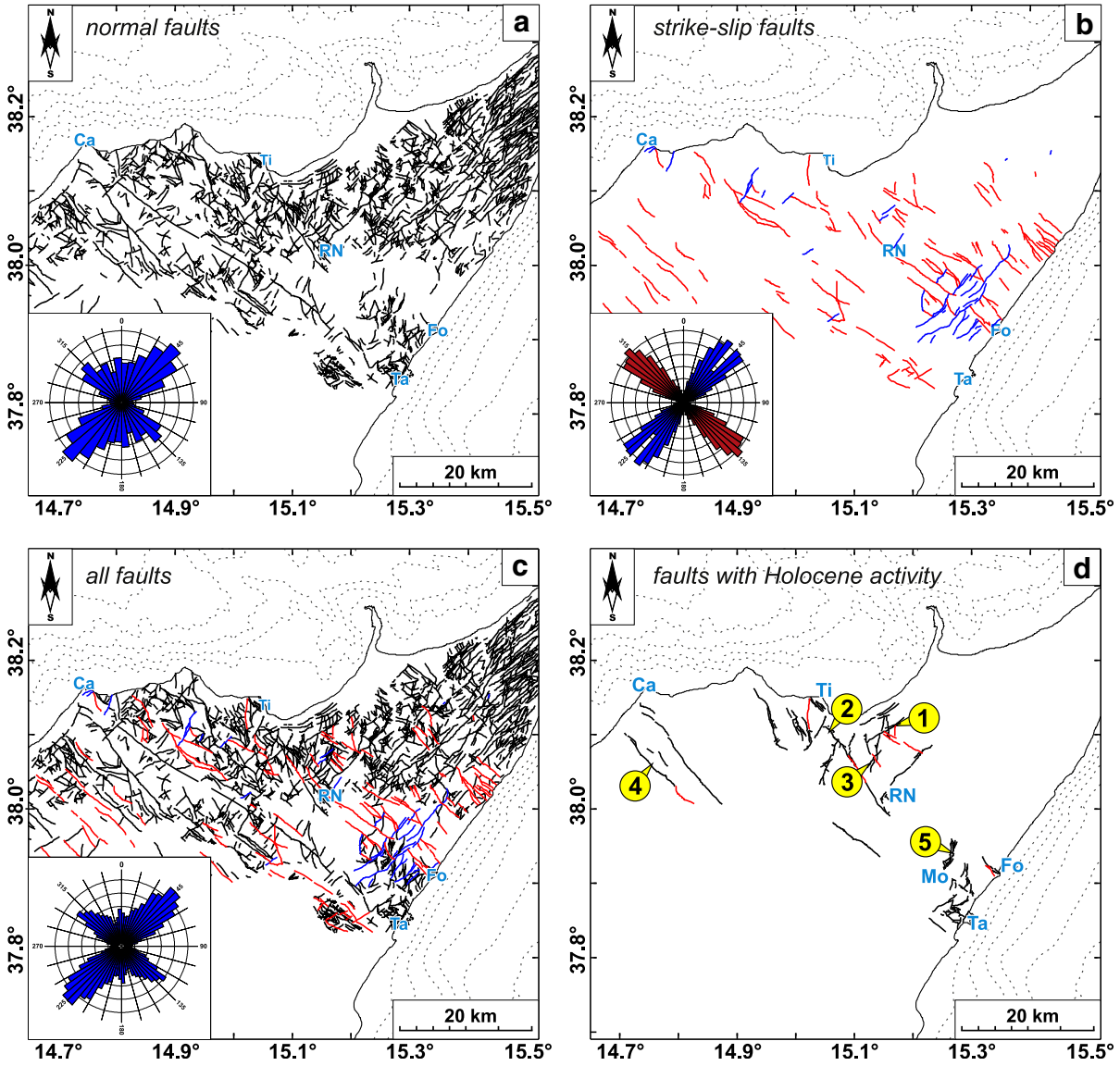

Fig. 7. Maps of the faults lying in the study area with prevailing dip–slip (a), and strike–slip (b) behaviour. In (b), faults are reported as red and blue lines for right-lateral and left-lateral strike–slip, respectively. c) Overall view of the faults displayed in panels a) and b). In each panel, a rose diagram showing the azimuth distribution of the structures is also shown. d) Map of faults with clear evidence of Holocene activity (numbers refer to photos reported in Fig. 8). RN = Rocca Novara; Mo = Mongiuffi; Fo = Forza D'Agro; Ta = Taormina.

4. Joint evaluation of results and discussion

In this section, we compare geodetic and geological observations (the latter mainly based on a compilation of published data), enabling characterizing the shallower expression of faults outcropping on the studied area. We go on to analyse the crustal features, using seismological and gravimetric data in order to obtain a more comprehensive understanding of the structural setting of study area.

4.1. Surface observations

4.1.1. Geological observations

After consulting all the available geological maps at 1:25.000/1:50.000 scales (Carbone et al., 1993, 1994, 1998; Lentini et al., 2000) and the recent literature (Billi et al., 2006; Catalano et al., 2009, 2012; De Guidi et al., 2013; Ghisetti, 1979; Hippolyte and Bouillin, 1999), we compiled a detailed map of all the faults that outcrop in the investigated area. We made different plots by distinguishing the faults according to their prevailing kinematics (Fig. 7) to better recognize patterns related to their areal distribution. In addition, all the faults for which detailed geological observations provided clear evidence of Holocene activity have been reported in Fig. 7d (see also Fig. 8 for some examples). It should be noted that we also included in this latter compilation faults that developed in Miocene times, during the nucleation of the Maghrebian fold and thrust-system and has been reactivated in Holocene times under a different stress field (e.g. Fig. 8b,d). Furthermore, this last compilation must be considered with caution because very few geological studies, focusing on these faults at a detailed scale, have been carried out. This implies that the compilation of the faults with Holocene activity may be incomplete because several faults may have been classified as not active during the Holocene due to the lack of detailed geological studies. In addition, from this analysis we have

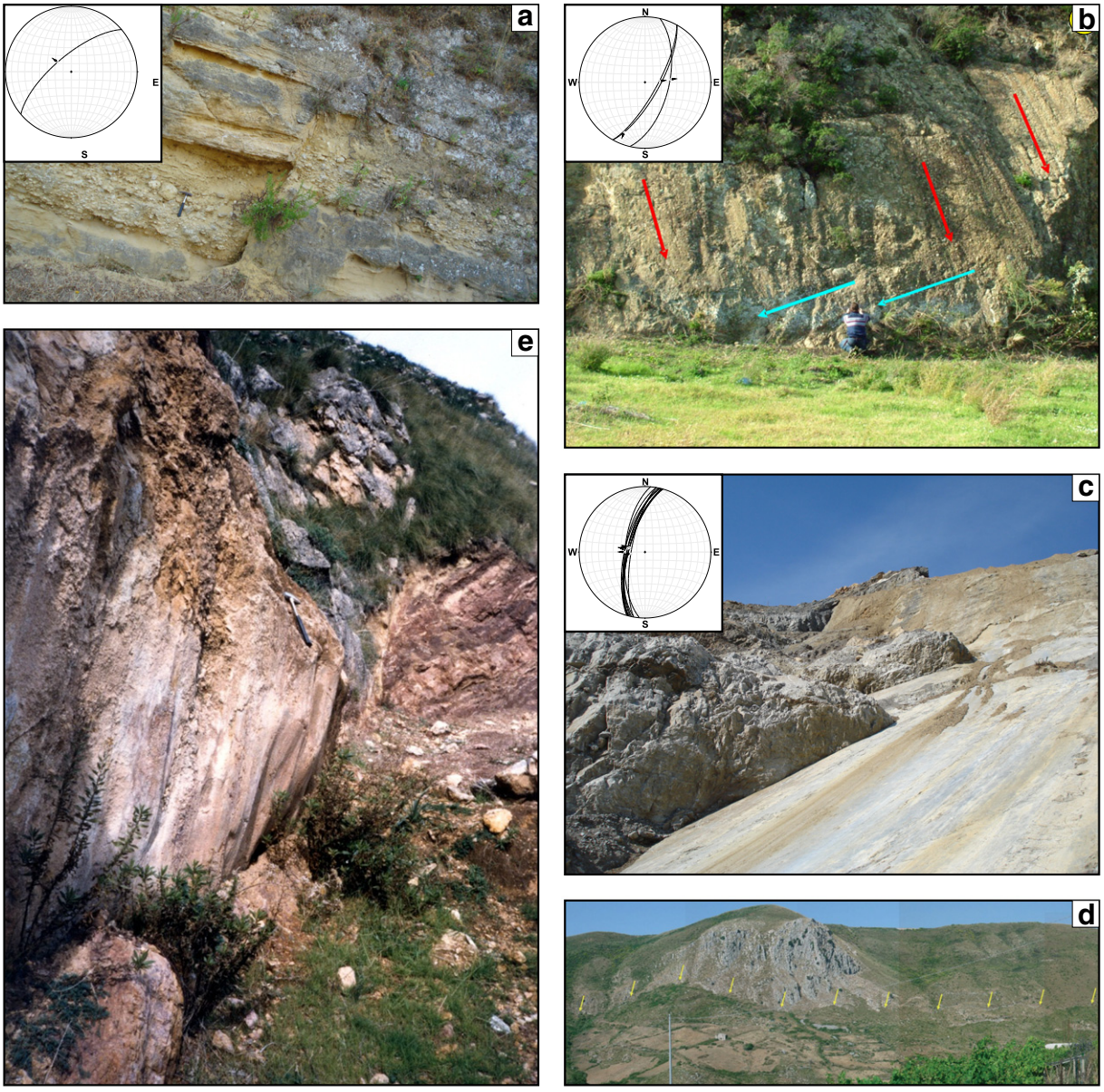

Fig. 8. Examples of faults characterized by activity during the Holocene. a) Normal fault cutting the metamorphic rocks of the chain and the current fluvial-coast deposits (stop 1 in Fig. 7d). The fault plane shows double sets of striations with normal dip–slip striae overprinting the right strike–slip ones (redrawn from De Guidi et al., 2013). b) Normal fault cutting the Pliocenic sedimentary rocks (stop 2 in Fig. 7d). c) Normal fault cutting the metamorphic rocks of the chain (stop 3 in Fig. 7d). d) Panoramic view of a rejuvenated free face along a NW–SE fault (stop 4 in Fig. 7d; redrawn from Catalano et al., 2012). e) Left stepping en échelon scarps of a subvertical fault cutting the carbonate rocks belonging to the Taormina Unit (stop 5 in Fig. 7d; courtesy of Raffaele Azzaro).

excluded all tectonic thrusts, since they are considered mostly inactive in this sector of Sicily starting from mid-Pleistocene times (Lanzafame and Bousquet, 1997; Lanzafame et al., 1997).

The presence of numerous faults with prevailing normal dip–slip kinematics is a key feature of the area. The rose diagram related to the azimuth distribution of normal faults (Fig. 7a) shows two main trends: a prevailing one striking N45°E and a secondary one aligned to the N130°E orientation. The former largely dominates the eastern sector of Peloritani Mts., while the latter can easily be recognized along the ATLFS and on the Nebrodi Mts. The right-lateral strike–slip faults represent the secondary tectonic feature of the area (red lines in Fig. 7b). These faults are prevailingly aligned N130°E and can be recognized on a large area which includes both the Nebrodi Mts. and the southeastern sector of Peloritani Mts. Notably, these faults are not present in the northeastern sector of the Peloritani Mts. The left-lateral strike–slip faults are recognizable only in the southeastern sector of the Peloritani Mts., close to the Ionian coast, and are characterized by a prevailing N45°E attitude (blue lines in Fig. 7b).

Summarizing, normal faults dominate the northern sector of the investigated onshore area (above a latitude of 38°N), while strike–slip faults tend to dominate the southern sector. In this picture, the central sector of ATLFS, mainly characterized by normal faulting and secondarily by right lateral ones (Fig. 8b; for additional details see also Ghisetti, 1979; Billi et al., 2006; De Guidi et al., 2013), seems connected southeastward to a ~N130°E oriented ca. 20-km-long right-lateral strike–slip set of faults (Fig. 7c). This last fault system, extending from Rocca Novara to the Ionian coast, seems to be disturbed by the already mentioned group of NE-striking left-lateral strike–slip faults. In any case, southeast of this crossing area, right-lateral active fault segments oriented N130°E and extending up to the coastal area, close to Forza D'Agrò ("Fo" in Fig. 7c), can again be identified (Fig. 8e; Ghisetti, 1979; Hippolyte and Bouillin, 1999).

To the west, a 10-km-wide belt aligned along the N130°E direction (Fig. 7c) of normal and right-lateral strike–slip faults connects the Tyrrhenian coast (close to Capo D'Orlando; "Ca" in Fig. 7c) to the Ionian coast (close to Taormina; "Ta" in Fig. 7c). Close to the northwestern sector of this belt, discrete segments of a NW–SE oriented dextral shear zone have been reactivated by extensional stress during the Holocene, accounting for up to 0.6 mm/yr of slip-rate (Fig. 8d; Catalano et al., 2012). This belt, known in literature as "Taormina Fault System" (TFS) and developed about 2 Myr ago (see Guarnieri, 2006; Rosenbaum et al., 2008 and references therein) seems to bound the southern tips of the N45°E left-lateral strike–slip faults. Overall, the set of faults including the TFS and the ATLFS (Fig. 7c) is believed to have accommodated the SSE-ward advance of the Calabro-Peloritan Arc with respect to the Sicilian block in response to the rollback of the Ionian subducting slab (e.g. Govers and Wortel, 2005; Neri et al., 2009; Rosenbaum et al., 2008).

4.1.2. Geodetic observations

As explained above, the geodetic velocity field is characterized by a general N-directed motion with a fan-shaped pattern, with the western sites located on Nebrodi Mts. diverging from the eastern ones located on Peloritani Mts (Fig. 6a). Divergence across the central sector of ATLFS can clearly be detected (Fig. 6a). By applying a vector decomposition of these velocities, Palano et al. (2012) estimated about 3.6 mm/yr of motion along the N126°E direction, resulting in dextral transtension on this NNW–SSE-striking segment of the ATLFS. The presence of some dextral strike–slip FPSs in the same area (Figs. 5b and 9a) matches well with the right-lateral shear component of the overall transtensional kinematics resulting from GNSS measurements. In the central sector of ATLFS, the strain-rate field (Fig. 6b) shows a prevailing NW–SE to NNW–SSE extension (up to 370 nanostrain/yr). This finding agrees with dominant normal faulting detected by structural data (Fig. 7a) and local earthquake FPSs (Figs. 5b and 9a) in the same area. In particular, FPSs show normal faulting on dislocation planes mainly oriented NE, in agreement with the prevailing strike of the extensional faults outcropping in the area. Overall, the N–S and N45°E faults define a releasing bend, which could represent the linkage between the central and the northern segments of the ATLFS.

West of the central sector of ATLFS, the strain-rate field shows a prevailing ENE–WSW extension (~220 nanostrain/yr), which rotates to a mainly N–S extension in the northern sector of the TFS and to WNW–ESE extension to the south. These last features are in agreement with the ones depicted by geological data (Catalano et al., 2012). Along the southern sector of ATLFS the strain-rate field displays a shear-dominated pattern since the principal extensional and contractional strain-rate axes have similar magnitudes (e.g. Holt and Haines, 1993). Indeed, the diverging motion of MNGR and 9532 sites with respect to TAOR and MMME (these stations move similarly to those located east of the ATLFS; Fig. 6a) suggests the presence of a deformation belt characterized by more than 1 mm/yr of right-lateral motion on the outcropping faults having a prevailing NW–SE attitude and referable to the ATLFS.

4.2. Crustal observations

The transition detected in the shallowest tomographic plates of Fig. 4 between (i) the high velocity domain of the southeastern Tyrrhenian and northeastern Sicily and (ii) the low-velocity one of the southwestern part of the study area, shows a fairly good spatial correspondence with the set including the TFS and ATLFS (Fig. 7c). This suggests that such TFS-ATLFS set may reasonably represent a crustal boundary between two different tectonic units marked by the seismic velocity domains. The evidence of this discontinuity between a northeastern high-velocity domain and a southwestern low-velocity one decreases when depth increases (Fig. 4), until the direction of the horizontal gradient of seismic velocity becomes N–S at 20 km depth and an east-trending low-velocity belt appears evident from the same 20 km-depth tomographic plate and from the deeper one (25 km). The east-trending low-velocity belt reasonably includes portions of different tectonic units of comparable seismic velocity, such as the easternmost part of mainland Sicily in the western portion of the belt, and the shallowest portion of the Ionian subducting slab in the eastern one. In this sector, the top of the Ionian subducting slab under the overriding southeastern Tyrrhenian unit, has been localized at a depth of the order of 20–25 km by previous investigators (e.g. Barberi et al., 2004; Cassinis et al., 2005; Orecchio et al., 2011).

Excluding the dense cloud of earthquakes located in the Mt. Etna volcanic area (Figs. 5a and 9b), most of the local seismicity during the study period has affected the central Aeolian Islands and the sector comprising the northern and central segments of the TFS and the ATLFS (Figs. 5a and 9b). The southern segments of TFS and ATLFS, between the Peloritani Mts. watershed and the Ionian coast, are characterized by substantial lack of seismicity that concurs with the lack of historical seismicity in the same area (Fig. 1b). A group of ~SE-trending right-lateral strike–slip faults, referable to the southern segment of the ATLFS, can be distinguished in the area of nil seismicity between the Peloritani Mts. and the Ionian coast of Sicily (Fig. 7b). Although no geological study proves the Holocene activity of this fault group with any certainty, the local ground deformation detected by geodetic data does suggest its activity at present. To the southeast, in the Ionian offshore (Fig. 1b), the occurrence of seismic activity associated with a transtensional faulting regime along a SE-trending belt (Fig. 5; see also Scarfì et al., 2009; D'Amico et al., 2010; Presti et al., 2013; Orecchio et al., 2014) reveals the existence of an active crustal shear zone which could represent the offshore continuation of the ATLFS. The location and kinematics of this seismogenic shear zone link to a system of NW–SE to WNW–ESE trending structures (Fig. 1a) inferred by multichannel seismic marine surveys carried out in recent decades along the Ionian offshore (e.g. Argnani and Bonazzi, 2005; Gallais et al., 2013; Nicolich et al., 2000; Polonia et al., 2011, 2012).

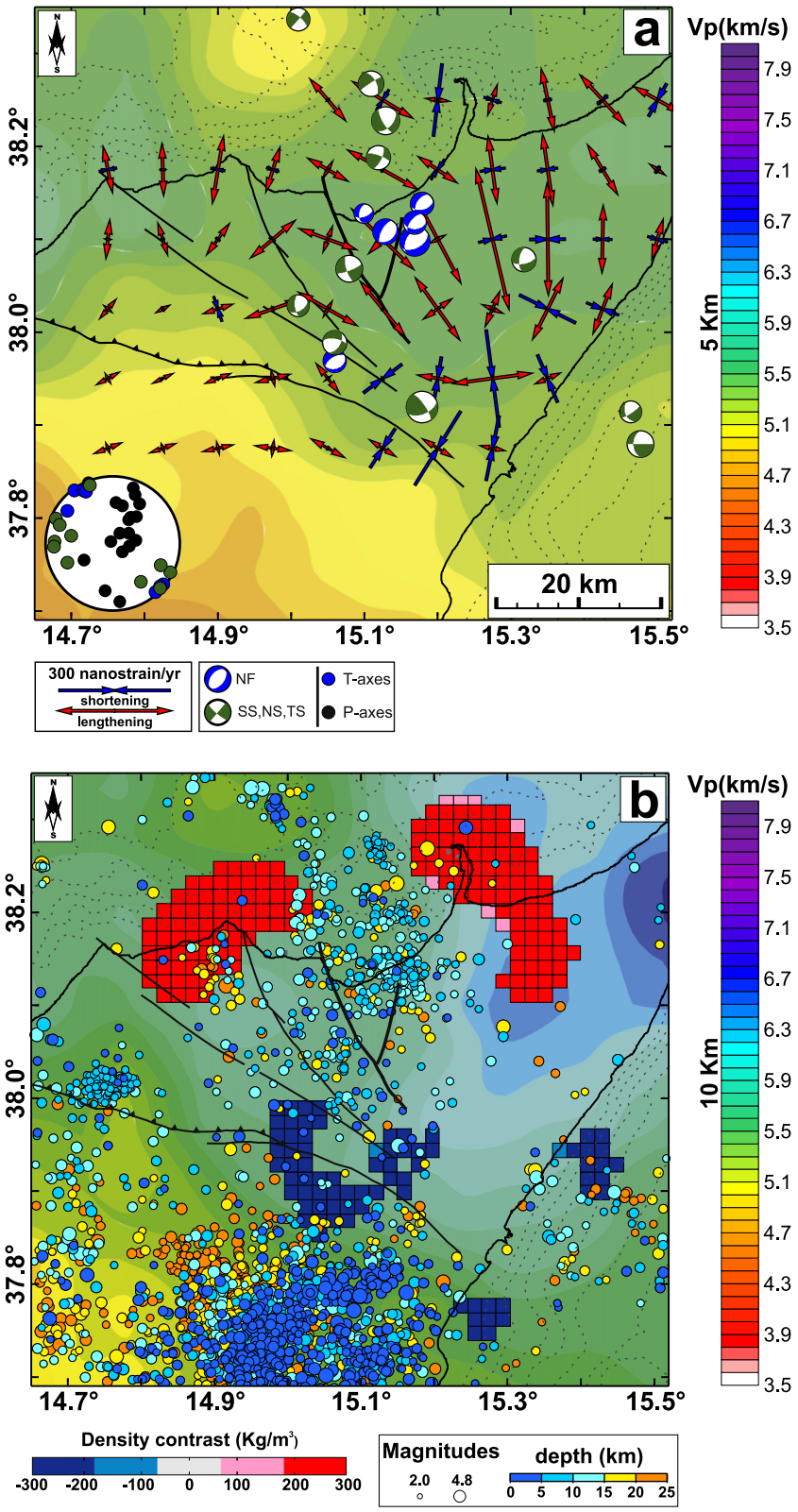

Fig. 9. Summary maps reporting: a) P-wave velocity distribution at 5 km depth, focal mechanisms estimated by waveform inversion and relative polar plot of P- and T-axes, and strain-rate field; b) P-wave velocity distribution at 10 km depth, epicentres of shallow earthquakes, and sectors of major density contrast detected at 9 km depth.

The coexistence in the investigated belt running from the Aeolian Islands to the Ionian offshore of normal and right-lateral strike–slip mechanisms with T-axes oriented NNW–SSE and WNW–ESE, respectively (blue and green dots in the polar plot of Fig. 9a), is compatible with the kinematics at the border of the overriding plate in a subduction trench retreat scenario. This has, in effect, been put forward as the geodynamic scenario of our study area, with the Southern Tyrrhenian–northeastern Sicily crust overthrusting onto the Ionian

subducting slab and moving laterally with respect to the confining crustal structure of mainland Sicily (Gallais et al., 2013; Neri et al., 2012; Palano et al., 2012; Polonia et al., 2011). Our data indicate that the dislocation of the overriding unit with respect to mainland Sicily occurs in our study area and is primarily located around the ATLFS. Also, as often observed worldwide in these kinds of processes (Bilich et al., 2001; Govers and Wortel, 2005; Wortel et al., 2009), the southeastward drifting of the overriding unit onto the subducting slab is affected by some degree of mechanical heterogeneity witnessed by the already discussed mechanism heterogeneity (Fig. 9a). It is also worth noting that both WNW-trending T-axes of strike–slip mechanisms (marking lateral motion at the border of the overriding unit) and NNW-trending T-axes of normal-faulting mechanisms (marking extension parallel to trench retreat in the same shear zone) may well be related to the primary geodynamic engine of subduction slab rollback.

4.3. Density and P-wave velocity correlation

The simple visual comparison between the spatial distribution of the modelled density contrast (Fig. 3) and the 3-D V_P model (Fig. 4) suggests that there is a certain degree of correlation between the two parameters. Low-velocity domains are generally characterized by negative density contrast (i.e. low density values), and conversely the high-velocity domains correspond to positive density contrast (i.e. high density values; Fig. 9b). Indeed, such correlation has previously been observed by Punturo et al. (2005). In particular, by performing petrophysical measurements on lithotypes outcropping in the eastern part of Peloritani Mts., these authors observed a clear tendency for a linear increase with densities of P-wave velocities, as commonly established by laboratory measurements. In order to evaluate such correlation, we converted the density contrasts in density values by considering a reference density of 2670 kg/m^3, generally assumed as the mean density value of surface continental rocks (Hinze, 2003). Although our modelled density and P-wave velocity values represent average values for each prismatic volume, they match well with those measured by Punturo et al. (2005), allowing us (i) to validate our modelled values and (ii) to associate these values to the main lithotypes outcropping in the investigated area, at least for shallow depths. In light of this, the high-grade metamorphic rocks belonging to the Hercynian basement, extensively outcropping in the northern sector of the investigated area are characterized by middle-to-high density/velocity values, while both sedimentary successions and low- to middle-grade metamorphic rocks, outcropping in the southern sector of the area, are characterized by low density/velocity values. Furthermore, taking into account the main results coming from the CROP project (Finetti, 2005), the above relationship between lithotypes and density/velocity values can be extended to the entire upper crust (see Fig. 5 and Fig. 11a in Del Ben et al., 2005 for additional details).

Looking at the V_P (Fig. 4) and density (Fig. 3) patterns, it appears that the crustal earthquake distribution is often concentrated in the areas characterized by middle to high V_P/density values (Fig. 9b). This aspect, coupled with the areal distribution of the outcropping lithotypes and their depth distribution (based on the CROP results; see Del Ben et al., 2005 for details), allows supposing a different rheological behaviour of the crust. In particular, we presume that areas characterized by middle-to-high V_P/density values (prevailing formed by high-grade metamorphic rocks) deform in a brittle manner and may produce appreciable seismic release. The areas characterized by low V_P/density values (mainly formed by sedimentary rocks) may behave in a more ductile manner and deformation may therefore occur aseismically. These considerations could eventually explain the lack of seismicity in the sector comprised between the Peloritani Mts. watershed and the Ionian coast (e.g. the southern sector of ALTFS), lending credence to a possible ductile behaviour of the crust in this sector of the investigated area. However, the dataset reported here does not provide strong quantitative support and further studies would be needed to address this hypothesis.

5. Geodynamic interpretation of the results

The transition between the two main seismic velocity domains detected by Local Earthquake Tomography in the upper 15 km of the study area (domains that we associate with the high-velocity Southern Tyrrhenian tectonic unit and low-velocity mainland Sicily, respectively) matches well with the set of faults comprising two SE-striking regional fault systems crossing northeastern Sicily, e.g. the Taormina Fault System (TFS) and the Aeolian–Tindari–Letojanni Fault System (ATLFS). Our multidisciplinary analysis reveals that this transitional zone is active in terms of seismicity and crustal deformation, showing some variation of seismic strain and faulting style along it. In particular, the greatest deformation and highest number of earthquakes are found in the northern and central sectors of ATLFS, low activity is detected along TFS, while a lack of seismicity (both recent and historical) is observed in the southern sector of ATLFS where, however, geodetic data reveal significant deformation. The geodetic, seismological and geologic data available along the ATLFS indicate changes in deformation style from prevailing dextral lateral-slip in the northern sector (Aeolian-Gulf of Patti), to primary normal faulting with minor dextral lateral-slip in the central sector (Tindari–Peloritani), and to mainly dextral lateral-slip again in the southern sector (Peloritani–Letojanni).

It is worth noting that the detected transitional zone between the two above discussed crustal domains correlates well with the southern edge of the Ionian subducting slab, as can clearly be recognized in upper mantle tomographic images (e.g. Neri et al., 2009 and references therein). The results of the present study match closely with the most widely accepted geodynamic model of the study region and may contribute to a more detailed definition of it in the area under investigation. In the current model, the progressive SE-ward rollback of the Ionian subducting slab was accommodated by the development of near-parallel right-lateral shear zones which, bordering the forearc–backarc system over time, have migrated eastward (see Billi et al., 2010 and references therein for details). In this framework, the TFS may represent the shallow expression of a lithospheric right-lateral shear zone formed about 2 Myr ago (Guarnieri, 2006): according to the findings of our study, this structure appears to be virtually inactive today. Conversely, our data seem to suggest that the ATLFS (described by previous investigators as the easternmost and youngest shear zone developed since the Middle–Late Pleistocene; Ghisetti, 1979; Finetti et al., 1996; Rosenbaum and Lister, 2004) is still active today and continues to accommodate the relative motion between the eastern extensional domain produced by subducting slab rollback and the western collisional one of mainland Sicily. It is also worth noting that our dataset, including good-quality locations and fault-plane solutions of offshore earthquakes, suggests the structural and kinematic southeastward continuation of the ATLFS into the Ionian Sea until joining with the faults cutting the Ionian accretionary wedge reported by Polonia et al. (2011, 2012). Based on multichannel and single-channel seismic profiles and bathymetric surveys, these authors provided clear evidence that a SE-striking deformation zone (Fig. 1a) separates the Ionian accretionary wedge in two lobes and accommodates the right-lateral differential movements between them. The same authors noted that the eastern lobe corresponds to the area of Calabro-Peloritan Arc where upper mantle tomography infers the presence of a continuous slab penetrating into the mantle, while the western lobe corresponds to areas where the slab appears already detached (Neri et al., 2009).

Our data and the deductions we have made imply the existence of a ~400-km-long highly segmented crustal shear zone extending from the Aeolian Islands up to the Ionian Abyssal plain, separating the domain of the Calabro-Peloritan Arc (east) from the Western-Central Sicily (west). The detected right-lateral transtensional kinematics, with a certain degree of heterogeneity along the shear zone, leads us to believe that

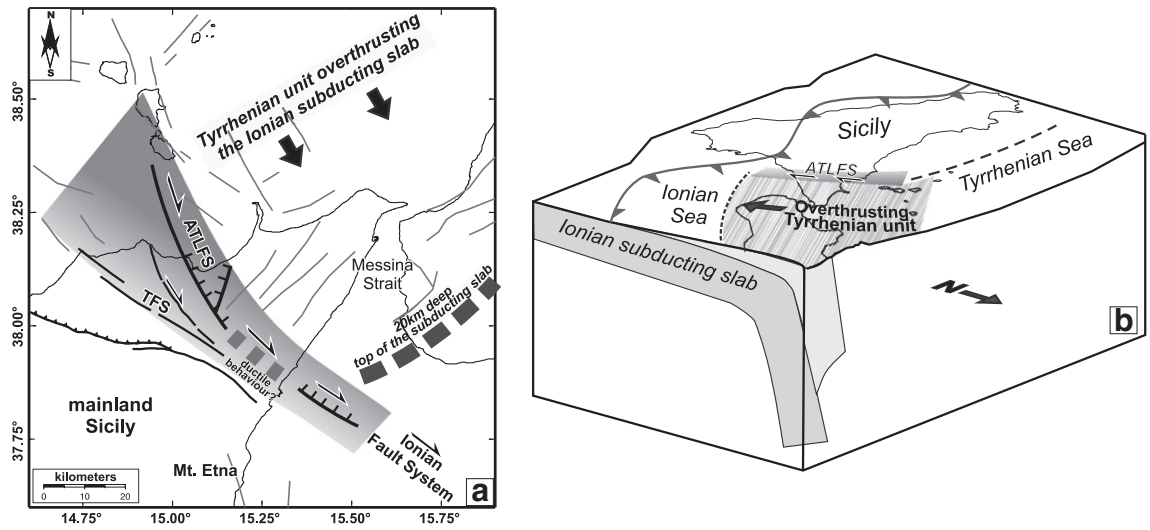

Fig. 10. Planimetric (a) and 3D (b) schematic views of our reconstruction of the shallow geodynamics at the southwestern edge of the Ionian subducting slab. The residual rollback of the slab drives the southeast-ward drifting of the Tyrrhenian overriding unit and provokes non-uniform transform motion of the latter on the ATLFS (Aeolian–Tindari–Letojanni Fault System) with respect to the laterally confining Sicily unit. The role of transtensional active boundary between the Tyrrhenian and Sicily units played by the ATLFS is indicated by seismic activity, ground deformation and geologic data, combined with crustal structure variation across it inferred from local earthquake tomography and gravity analysis.

this probably acts as already observed on the edges of retreating subduction slabs. In other words, where the overriding plate driven by trench retreat moves w.r.t. the laterally confining plate with a highly non-uniform transform motion (see e.g. Govers and Wortel, 2005). In the main study area of this work, the high-V_P Southern Tyrrhenian overriding unit is detected in the upper 15 km while, at 20–25 km depth below its most advanced front (Messina Straits), relatively low-V_P marks the top of the Ionian subducting slab and confirms our reconstruction (Fig. 10). Wider scale investigations over the entire domain of the Tyrrhenian subduction zone are required for more exhaustive modelling of the geodynamic process.

6. Concluding remarks

Seismic activity, ground deformation and geologic data, combined with crustal structure inferred from seismic tomography and gravity analysis, show that the Tyrrhenian and Calabro-Peloritan Arc unit is moving southeastward with respect to Western-Central Sicily, and this relative motion is mainly accommodated by the Aeolian–Tindari–Letojanni Fault System (ATLFS) with highly non-uniform right-lateral transtensional kinematics. Seismic data suggest the structural and kinematic continuation of ATLFS in the Ionian sea until joining up with the system of faults reported by previous researchers and separating the Ionian accretionary wedge in two lobes: (i) an eastern lobe corresponding to the Calabro-Peloritan Arc domain where previous upper mantle tomography highlighted the presence of a continuous slab penetrating into the mantle and (ii) a western one corresponding to sectors where the slab appears already detached.

The observed features of the ATLFS with its continuation in the Ionian Sea, jointly with other information from literature concerning the shallow-to-deep structure and the geodynamics of the study region, lead us to recognize a broad highly-segmented shear zone extending from the Aeolian Islands to the Ionian Abyssal plain, separating the eastern extensional domain of Calabro-Peloritan Arc from the western collisional one of Sicily (Fig. 10). In our reconstruction, the residual motion of rollback of the Ionian subducting slab (the top of which is detected at a depth of 20–25 km beneath the advanced front of the Tyrrhenian unit) drives the southeast-ward drifting of the Tyrrhenian overriding unit and provokes non-uniform transform motion of this on the ATLFS and its Ionian continuation with respect to the laterally confining Sicily unit.

Acknowledgments

We thank the Editor-in-Chief Kelin Wang and two anonymous reviewers for their critical reviews, constructive suggestions and useful comments that greatly helped improving the paper. We are grateful to Raffaele Azzaro for providing the photo in Fig. 8. This research has benefited from funding provided by PO-FESR 2007/2013 Project 'Attività di sviluppo sperimentale finalizzata allariduzione del rischio sismico nella Sicilia Orientale'. We thank S. Conway for correcting and improving the English language of this paper.

Appendix A. Supplementary data

Supplementary data to this article can be found online at http://dx.doi.org/10.1016/j.tecto.2015.07.005.

References

Anderson, H.J., Jackson, J.A., 1987. The deep seismicity of the Tyrrhenian sea. Geophys. J. Int. 91, 613–637. http://dx.doi.org/10.1111/j.1365-246X.1987.tb01661.x.
Argnani, A., 2014. Comment on the article "Propagation of a lithospheric tear fault (STEP) through the western boundary of the Calabrian accretionary wedge offshore eastern Sicily (Southern Italy)" by Gallais et al., 2013 Tectonophysics. Tectonophysics 610, 195–199. http://dx.doi.org/10.1016/j.tecto.2013.06.035.
Argnani, A., Bonazzi, C., 2005. The Malta Escarpment fault zone offshore eastern Sicily: Pliocene–Quaternary tectonic evolution based on new multichannel seismic data. Tectonics 24, TC4009. http://dx.doi.org/10.1029/2004TC001656.
Argnani, A., Serpelloni, E., Bonazzi, C., 2007. Pattern of deformation around the central Aeolian Islands: evidence from GPS data and multichannel seismics. Terra Nova 19, 317–323.
Azzaro, R., Bernardini, F., Camassi, R., Castelli, V., 2007. The 1780 seismic sequence in NE Sicily (Italy): shifting an underestimated and mislocated earthquake to a seismically low rate zone. Nat. Hazards 42 (1), 149–167. http://dx.doi.org/10.1007/s11069-006-9066-1.
Ballarin, S., Palla, B., Trombetti, C., 1972. The Construction of the Gravimetric Map of Italy. Pubblicazioni della Commissione Geodetica Italiana, Terza Serie. I.G.M., Firenze (31 pp.).
Barberi, G., Cosentino, M.T., Gervasi, A., Guerra, I., Neri, G., Orecchio, B., 2004. Crustal seismic tomography in the Calabrian arc region, south Italy. Phys. Earth Planet. Inter. 147, 297–314. http://dx.doi.org/10.1016/j.pepi.2004.04.005.
Bilich, A., Frohlich, C., Mann, P., 2001. Global seismicity characteristics of subduction-to-strike–slip transitions. J. Geophys. Res. 106, 19,443–19,452. http://dx.doi.org/10.1029/2000JB900309.
Billi, A., Barberi, G., Faccenna, C., Neri, G., Pepe, F., Sulli, A., 2006. Tectonics and seismicity of the Tindary Fault System, southern Italy: crustal deformations at the transition between ongoing contractional and extensional domains located above the edge of a subducting slab. Tectonics 25, 1–20.

Billi, A., Presti, D., Faccenna, C., Neri, G., Orecchio, B., 2007. Seismotectonics of the Nubia plate compressive margin in the south-Tyrrhenian region, Italy: clues for subduction inception. J. Geophys. Res. 112, B08302. http://dx.doi.org/10.1029/2006JB004837.

Billi, A., Presti, D., Orecchio, B., Faccenna, C., Neri, G., 2010. Incipient extension along the active convergent margin of Nubia in Sicily, Italy: Cefalù–Etna seismic zone. Tectonics 29, TC4026. http://dx.doi.org/10.1029/2009TC002559.

Camacho, A.G., Montesinos, F.G., Vieira, R., 2000. Gravity inversion by means of growing bodies. Geophysics 65 (1), 95–101.

Camacho, A.G., Montesinos, F.G., Vieira, R., 2002. A 3-D gravity inversion tool based on exploration of model possibilities. Comput. Geosci. 28, 191–204.

Camacho, A.G., Fernández, J., Gottsmann, J., 2011. The 3-D gravity inversion package GROWTH 2.0 and its application to Tenerife Island, Spain. Comput. Geosci. http://dx.doi.org/10.1016/j.cageo.2010.12.003.

Carbone, S., Catalano, S., Lentini, F., Vinci, G., 1993. Carta geologica del Golfo di Patti (Sicilia Settentrionale), Scala 1:25.000. S.EL.CA., Firenze.

Carbone, S., Catalano, S., Lentini, F., Vinci, G., 1994. Carta geologica dei Monti di Taormina (Monti Peloritani - Sicilia Nord-Orientale), Scala 1:25.000. S.EL.CA., Firenze.

Carbone, S., Lentini, F., Vinci, G., 1998. Carta geologica del settore occidentale dei Monti Peloritani, scala 1:25.000. S.EL.CA., Firenze.

Cassinis, R., Scarascia, S., Lozej, A., 2005. Review of seismic wide angle reflection-refraction (WARR) results in the Italian region (1956–1987). In: Finetti, I.R. (Ed.), CROP Project-Deep Seismic Exploration of the Central Mediterranean Region and ItalyAtlases in Geoscience vol. 1. Elsevier Earth and Environmental Science, New York, pp. 31–55.

Catalano, S., Romagnoli, G., Tortorici, G., 2009. The late Quaternary crustal deformation of NE Sicily: evidence for an active mantle diapirism. G.N.G.T.S., Abstracts of the 27° Assembly, pp. 152–154.

Catalano, S., Pavano, F., Romagnoli, G., Tortorici, G., 2012. Active tectonics along the Nebrodi-Peloritani boundary (NE Sicily): a new potential seismogenic source. G.N.G.T.S., Abstracts of the 30° Assembly, pp. 29–33.

Cuffaro, M., Riguzzi, F., Scrocca, D., Doglioni, C., 2011. Coexisting tectonic settings: the example of the southern Tyrrhenian Sea. Int. J. Earth Sci. (Geol. Rundsch.) 100 (8), 1915–1924. http://dx.doi.org/10.1007/s00531-010-0625-z.

D'Amico, S., Orecchio, B., Presti, D., Zhu, L., Herrmann, R.B., Neri, G., 2010. Broadband waveform inversion of moderate earthquakes in the Messina Straits, southern Italy. Phys. Earth Planet. Inter. 179, 97–106. http://dx.doi.org/10.1016/j. pepi.2010.01.012.

De Astis, G., Ventura, G., Vilardo, G., 2003. Geodynamic significance of the Aeolian volcanism (Southern Tyrrhenian Sea, Italy) in light of structural, seismological, and geochemical data. Tectonics 22 (4), 1040. http://dx.doi.org/10.1029/2003TC001506.

De Guidi, G., Lanzafame, G., Palano, M., Puglisi, G., Scaltrito, A., Scarfì, L., 2013. Multidisciplinary study of the Tindari Fault (Sicily, Italy) separating ongoing contractional and extensional compartments along the active Africa–Eurasia convergent boundary. Tectonophysics 588, 1–17. http://dx.doi.org/10.1016/j.tecto.2012.11.021.

Del Ben, A., De Luca, L., Finetti, I.R., Forlin, E., Luzio, D., Pipan, M., Prizzon, A., Vitale, M., 2005. Comparative NV and WA seismic modelling of sections in the Tyrrhenian Sea. In: Finetti, I.R. (Ed.), CROP PROJECT: Deep Seismic Exploration of the Central Mediterranean and Italy, pp. 377–392 (Chapter 16).

Dewey, J.F., Pitman, W.C., Ryan, W.B.F., Bonnin, J., 1973. Plate tectonics and the evolution of the Alpine system. Geol. Soc. Am. Bull. 84, 3137–3180.

Doglioni, C., 1993. Geological evidence for a global tectonic polarity. J. Geol. Soc. Lond. 150, 991–1002. http://dx.doi.org/10.1144/gsjgs.150.5.0991.

England, P., Molnar, P., 1997. Active deformation of Asia: from kinematics to dynamics. Science 278, 647–650. http://dx.doi.org/10.1126/science.278.5338.647.

Evans, J.R., Eberhart-Phillips, D., Thurber, C.H., 1994. User's manual for simulps12for imaging VP and VP/VS: a derivative of the 'Thurber' tomographic inversion simul3 for local earthquakes and explosions. USGS Open-file Report 94-431.

Faccenna, C., Becker, T.W., Lucente, F.P., Jolivet, L., Rossetti, F., 2001. History of subduction and back-arc extension in the central Mediterranean. Geophys. J. Int. 145, 809–820. http://dx.doi.org/10.1046/j.0956-540X.2001.01435.x.

Faccenna, C., Piromallo, C., Crespo-Blanc, A., Jolivet, L., Rossetti, F., 2004. Lateral slab deformation and the origin of western Mediterranean arcs. Tectonics 23, TC1012. http://dx.doi.org/10.1029/2002TC001488.

Favalli, M., Karátson, D., Mazzuoli, R., Pareschi, M.T., Ventura, G., 2005. Volcanic geomorphology and tectonics of the Aeolian archipelago (Southern Italy) based on integrated DEM data. Bull. Volcanol. 68 (2), 157–170. http://dx.doi.org/10.1007/s00445-005-0429-3.

Finetti, I.R., 2005. CROP Project, Deep Seismic Exploration of the Central Mediterranean and Italy. Elsevier B.V. (794 pages).

Finetti, I., Lentini, F., Carbone, S., Catalano, S., Del Ben, A., 1996. Il Sistema Appennino Meridionale-Arco Calabro-Sicilia nel mediterraneo centrale: studio geologico-geofisico. Mem. Soc. Geol. It. 115, 529–559.

Frepoli, A., Amato, A., 2000. Fault plane solutions of crustal earthquakes in Southern Italy (1988–1995): seismotectonic implications. Ann. Geophys. 43 (3), 437–467.

Gallais, F., Graindorge, D., Gutscher, M.A., Klaeschen, D., 2013. Propagation of a lithospheric tear fault (STEP) through the western boundary of the Calabrian accretionary wedge offshore eastern Sicily (Southern Italy). Tectonophysics 602, 141–152. http://dx.doi.org/10.1016/j.tecto.2012.12.026.

Gambino, S., Milluzzo, V., Scaltrito, A., Scarfì, L., 2012. Relocation and focal mechanisms of earthquakes in the south-central sector of the Aeolian Archipelago: new structural and volcanological insights. Tectonophysics 524–525, 108–115. http://dx.doi.org/10.1016/j.tecto.2011.12.024.

Ghisetti, F., 1979. Relations between structure and transcurrent and distensive phases in the Messina–Fiumefreddo, Tindari–Letojanni and Alia–Malvagna systems (northeastern Sicily); a microtectonic study. Geol. Romana 18, 23–58.

Giammanco, S., Palano, M., Scaltrito, A., Scarfì, L., Sortino, F., 2008. Possible role of fluid overpressure in the generation of earthquake swarms in active tectonic areas: the case of the Peloritani Mts. (Sicily, Italy). J. Volcanol. Geotherm. Res. 178, 795–806. http://dx.doi.org/10.1016/j.jvolgeores.2008.09.005.

Giunta, G., Luzio, D., Agosta, F., Calò, M., Di Trapani, F., Giorgianni, A., Oliveri, E., Orioli, S., Perniciaro, M., Vitale, M., Chiodi, M., Adelfio, G., 2009. An integrated approach to investigate the seismotectonics of northern Sicily and southern Tyrrhenian. Tectonophysics 476, 13–21. http://dx.doi.org/10.1016/j.tecto.2008.09.031.

Goes, S., Giardini, D., Jenny, S., Hollenstein, C., Kahle, H.-G., Geiger, A., 2004. A recent reorganization in the south-central Mediterranean. Earth Planet. Sci. Lett. 226, 335–345. http://dx.doi.org/10.1016/j.epsl.2004.07.038.

Govers, R., Wortel, M.J.R., 2005. Lithosphere tearing at STEP faults: response to edges of subduction zones. Earth Planet. Sci. Lett. 236, 505–523. http://dx.doi.org/10.1016/j.epsl.2005.03.022.

Guarnieri, P., 2006. Plio-Quaternary segmentation of the south Tyrrhenian forearc basin. Int. J. Earth Sci. 95, 107–118. http://dx.doi.org/10.1007/s00531-005-0005-2.

Gueguen, E., Doglioni, C., Fernandez, M., 1998. On the post-25 Ma geodynamic evolution of the western Mediterranean. Tectonophysics 298, 259–269.

Herring, T.A., King, R.W., McClusky, S.C., 2010. Introduction to GAMIT/GLOBK, Release 10.4. Massachusetts Institute of Technology, Cambridge MA, pp. 1–48.

Hinze, W.J., 2003. Bouguer reduction density, why 2.67? Geophysics 68 (5), 1559–1560.

Hippolyte, J.C., Bouillin, J.P., 1999. Morphologie et cinématique d'une faille holocène dans les monts Péloritains (Sicile); implications géodynamiques. C.R. Acad. Sci., Ser. IIa: Earth Planet. Sci. 329, 741–747. http://dx.doi.org/10.1016/S1251-8050(00)88494-3.

Holt, W.E., Haines, A.J., 1993. Velocity fields in deforming Asia from the inversion of earthquake-released strains. Tectonics 12 (1), 1–20. http://dx.doi.org/10.1029/92TC00658.

Jolivet, L., Faccenna, C., Goffè, B., Mattei, M., Rossetti, F., Brunet, C., Storti, F., Funiciello, R., Cadet, J.P., D'Agostino, N., Parra, T., 1998. Midcrustal shear zones in postorogenic extension: example from the northern Tyrrhenian Sea. J. Geophys. Res. 103, 12123–12160. http://dx.doi.org/10.1029/97JB03616.

Lanzafame, G., Bousquet, J.C., 1997. The maltese escarpment and its extension from Mt. Etna to Aeolian Islands (Sicily): importance and evolution of lithosphere discontinuity. Acta Vulcanol. 9 (1/2), 113–120.

Lanzafame, G., Leonardi, A., Neri, M., Rust, D., 1997. Late overthrust of the Appenine–Maghrebian Chain at the NE periphery of Mt. Etna, Sicily. C.R. Acad. Sci., Ser. IIa 324, 325–332.

Lentini, F., Carbone, S., Grasso, M., 2000. Carta geologica della Provincia di Messina, scala 1:50.000 with illustrative notes. S.EL.CA., Firenze.

Malinverno, A., Ryan, W.B.F., 1986. Extension in the Tyrrhenian Sea and shortening in the Apennines as result of arc migration driven by sinking of the lithosphere. Tectonics 5 (2), 227–245. http://dx.doi.org/10.1029/TC005i002p00227.

Morelli, C., Gantar, C., Honkasalo, T., McConnel, R.K., Tanner, I.G., Szabo, B., Uotila, U., Whalen, C.T., 1974. The International Gravity Standardization Net 1971. International Association of Geodesy. Special Publication 4. IUGG 194.

Moritz, H., 1980. Geodetic Reference System 1980. Bull. Géod. 54, 395–405.

Musumeci, C., Scarfì, L., Palano, M., Patanè, D., 2014. Foreland segmentation along an active convergent margin: new constraints in southeastern Sicily (Italy) from seismic and geodetic observations. Tectonophysics 630, 137–149. http://dx.doi.org/10.1016/j.tecto.2014.05.017.

Neri, G., Barberi, G., Orecchio, B., Mostaccio, A., 2003. Seismic strain and seismogenic stress regimes in the crust of the southern Tyrrhenian region. Earth Planet. Sci. Lett. 213, 97–112. http://dx.doi.org/10.1016/S0012-821X(03)00293-0.

Neri, G., Barberi, G., Oliva, G., Orecchio, B., 2004. Tectonic stress and seismogenic faulting in the area of the 1908 Messina earthquake, south Italy. Geophys. Res. Lett. 31, L10602. http://dx.doi.org/10.1029/2004GL019742.

Neri, G., Barberi, G., Oliva, G., Orecchio, B., 2005. Spatial variations of seismogenic stress orientations in Sicily, south Italy. Phys. Earth Planet. Inter. 148, 175–191. http://dx.doi.org/10.1016/j.pepi.2004.08.009.

Neri, G., Oliva, G., Orecchio, B., Presti, D., 2006. A possible seismic gap within a highly seismogenic belt crossing Calabria and Eastern Sicily, Italy. Bull. Seismol. Soc. Am. 96, 1321–1331.

Neri, G., Orecchio, B., Totaro, C., Falcone, G., Presti, D., 2009. Subduction beneath southern Italy is close to ending: results from seismic tomography. Seismol. Res. Lett. 80, 63–70. http://dx.doi.org/10.1785/gssrl.80.1.63.

Neri, G., Marotta, A.M., Orecchio, B., Presti, D., Totaro, C., Barzaghi, R., Borghi, A., 2012. How lithospheric subduction changes along the Calabrian Arc in southern Italy: geophysical evidences. Int. J. Earth Sci. 101, 1949–1969.

Nicolich, R., Laigle, M., Hirn, A., Cernobori, L., Gallard, J., 2000. Crustal structure of the Ionian margin of Sicily: Etna volcano in the frame of regional evolution. Tectonophysics 329, 121–139. http://dx.doi.org/10.1016/S0040-1951(00)00192-X.

Orecchio, B., Presti, D., Totaro, C., Guerra, I., Neri, G., 2011. Imaging the velocity structure of the Calabrian Arc region (South Italy) through the integration of different seismological data. Boll. Geofis. Teor. Appl. 52, 625–638.

Orecchio, B., Presti, D., Totaro, C., Neri, G., 2014. What earthquakes say concerning residual subduction and STEP dynamics in the Calabrian Arc region, south Italy. Geophys. J. Int. 199 (3), 1929–1942. http://dx.doi.org/10.1093/gji/ggu373.

Palano, M., 2015. On the present-day crustal stress, strain-rate fields and mantle anisotropy pattern of Italy. Geophys. J. Int. 200 (2), 969–985. http://dx.doi.org/10.1093/gji/ggu451.

Palano, M., Ferranti, L., Monaco, C., Mattia, M., Aloisi, M., Bruno, V., Cannavò, F., Siligato, G., 2012. GPS velocity and strain fields in Sicily and southern Calabria, Italy: updated geodetic constraints on tectonic block interaction in the central Mediterranean. J. Geophys. Res. 117, B07401. http://dx.doi.org/10.1029/2012JB009254.

Palano, M., Imprescia, P., Gresta, S., 2013. Current stress and strain-rate fields across the Dead Sea Fault System: constraints from seismological data and GPS observations. Earth Planet. Sci. Lett. 369–370, 305–316. http://dx.doi.org/10.1016/j.epsl.2013.03.043.

Patacca, E., Sartori, R., Scandone, P., 1990. Tyrrhenian basin and Apenninic arcs. Kinematic relations since late Tortonian times. Mem. Soc. Geol. Ital. 45, 425–451.
Polonia, A., Torelli, L., Mussoni, P., Gasperini, L., Artoni, A., Klaeschen, D., 2011. The Calabrian Arc subduction complex in the Ionian Sea: regional architecture, active deformation, and seismic hazard. Tectonics 30, TC5018. http://dx.doi.org/10.1029/2010TC002821.
Polonia, A., Torelli, L., Gasperini, L., Mussoni, P., 2012. Active faults and historical earthquakes in the Messina Straits area (Ionian Sea). Nat. Hazards Earth Syst. Sci. 12, 2311–2328. http://dx.doi.org/10.5194/nhess-12-2311-2012.
Pondrelli, S., Piromallo, C., Serpelloni, E., 2004. Convergence vs. retreat in Southern Tyrrhenian Sea: insights from kinematics. Geophys. Res. Lett. 31 (6), L06611.
Pondrelli, S., Salimbeni, S., Ekström, G., Morelli, A., Gasperini, P., Vannucci, G., 2006. The Italian CMT dataset from 1977 to the present. Phys. Earth Planet. Inter. 286–303. http://dx.doi.org/10.1016/j.pepi.2006.07.008,159/3-4.
Presti, D., Troise, C., De Natale, G., 2004. Probabilistic location of seismic sequences in heterogeneous media. Bull. Seismol. Soc. Am. 94, 2239–2253.
Presti, D., Orecchio, B., Falcone, G., Neri, G., 2008. Linear versus non-linear earthquake location and seismogenic fault detection in the southern Tyrrhenian Sea, Italy. Geophys. J. Int. 172 (2), 607–618. http://dx.doi.org/10.1111/j.1365-246X.2007.03642.x.
Presti, D., Billi, A., Orecchio, B., Totaro, C., Faccenna, C., Neri, G., 2013. Earthquake focal mechanisms, seismogenic stress, and seismotectonics of the Calabrian Arc, Italy. Tectonophysics 602, 153–175. http://dx.doi.org/10.1016/j.tecto.2013.01.030.
Punturo, R., Kern, H., Cirrincione, R., Mazzoleni, P., Pezzino, A., 2005. P- and S-wave velocities and densities in silicate and calcite rocks from the Peloritani Mountains, Sicily (Italy): the effect of pressure, temperature and the direction of wave propagation. Tectonophysics 409, 55–72. http://dx.doi.org/10.1016/j.tecto.2005.08.006.
Rosenbaum, G., Lister, G.S., 2004. Neogene and Quaternary rollback evolution of the Tyrrhenian Sea, the Apennines and the Sicilian Maghrebides. Tectonics 23, TC1013. http://dx.doi.org/10.1029/2003TC001518.
Rosenbaum, G., Gasparon, M., Lucente, F.P., Peccerillo, A., Miller, M.S., 2008. Kinematics of slab tear faults during subduction segmentation and implications for Italian magmatism. Tectonics 27, TC2008. http://dx.doi.org/10.1029/2007TC002143.
Rovida, A., Camassi, R., Gasperini, P., Stucchi, M., 2011. CPTI11, the 2011 version of the Parametric Catalogue of Italian Earthquakes. Milano, Bologna. (http://emidius.mi.ingv.it/CPTI, http://dx.doi.org/10.6092/INGV.IT-CPTI11).
Scarfì, L., Langer, H., Scaltrito, A., 2009. Seismicity, seismotectonics and crustal velocity structure of the Messina Strait (Italy). Phys. Earth Planet. Inter. 177, 65–78. http://dx.doi.org/10.1016/j.pepi.2009.07.010.
Scognamiglio, L., Tinti, E., Michelini, A., 2009. Real-time determination of seismic moment tensor for the Italian Region. Bull. Seismol. Soc. Am. 99 (4), 2223–2242. http://dx.doi.org/10.1785/0120080104.
Ventura, G., Vilardo, G., Milano, G., Pino, N.A., 1999. Relationships among crustal structure, volcanism and strike–slip tectonics in the Lipari–Vulcano Volcanic Complex (Aeolian Islands, Southern Tyrrhenian Sea, Italy). Phys. Earth Planet. Inter. 116, 31–52.
Wessel, P., Bercovici, D., 1998. Interpolation with splines in tension: a Green's function approach. Math. Geol. 30, 77–93.
Westaway, R., 1990. Present-day kinematics of the plate boundary zone between Africa and Europe, from the Azores to Aegean. Earth Planet. Sci. Lett. 96, 392–406. http://dx.doi.org/10.1016/0012-821X(90)90015-P.
Wortel, M.J.R., Spakman, W., 2000. Subduction and slab detachment in the Mediterranean–Carpathian Region. Science 290, 1917–1920. http://dx.doi.org/10.1126/science.290.5498.1910.
Wortel, M.J.R., Govers, R., Spakman, W., 2009. Continental collision and the STEP-wise evolution of convergent plate boundaries: from structure to dynamics. In: Lallemand, S., Funiciello, F. (Eds.), Subduction Zone Geodynamics. Springer-Verlag, Berlin Heidelberg, pp. 47–59.

Web references

http://www.ingv.it, 2015/06/01
http://www.globalcmt.org 2015/06/01
http://www.bo.ingv.it/RCMT/searchRCMT.html 2015/06/01
http://zonesismiche.mi.ingv.it/ 2015/06/01